

Characterizing Attapulgite-Reinforced Nanocomposites of Poly(lactic acid)

Chi-Hui Tsou^{a,b,c,d,*}, Jipeng Guo^a, Ji-Ang Lei^e,
Manuel Reyes De Guzman^a, and Maw-Cherng Suen^{f,**}

^aSchool of Materials Science and Engineering, Sichuan University of Science and Engineering, Zigong, 643000 China

^bMaterial Corrosion and Protection Key Laboratory of Sichuan Province, Zigong, 643000 China

^cSichuan Zhixiangyi Technology Co., Ltd., Chengdu, 610051 China

^dDepartment of Materials Science, Chulalongkorn University, Bangkok, 10330 Thailand

^eGraduate School of Applied Technology, Taoyuan Innovation Institute of Technology, Jongli, 32091 Taiwan

^fDepartment of Fashion Business Administration, Lee-Ming Institute of Technology, New Taipei City, 24305 Taiwan

*e-mail: mayko0301@hotmail.com

**e-mail: sunmc0414@gmail.com

Received June 6, 2020; revised August 4, 2020; accepted August 7, 2020

Abstract—Attapulgite (ATT) is a naturally rigid reinforcing filler. In this present study, ATT was first purified, and varying amounts of purified ATT was added to polylactic acid (PLA) to modify PLA through a melt-blending technique. The objective was to determine how the content of ATT affected the characteristics of the ensuing PLA/ATT nanocomposites: morphology, mechanical and thermal properties. Filling PLA with ATT increased both the thermal and mechanical properties, but too much ATT was not beneficial as the effect was to decrease both properties. Energy dispersive spectroscopy indicated that the percentage of Si element increased with the amount of ATT, but more than 10 wt % ATT led to a poor ATT distribution in the nanocomposites.

DOI: 10.1134/S0965545X20330068

INTRODUCTION

Petroleum products are not friendly to the environment, and the problem with the pollution brought about by plastics is mounting [1]. For these reasons, a lot of research has been looking into biodegradable materials. There is a host of available biodegradable polymers, one of which is poly(lactic acid) (PLA). PLA can be obtained from plants. Its classification falls under the aliphatic polyesters, which are the thermoplastic type [2]. It is a rigid polymer at room temperature, and some of its properties are as follows: glass transition temperature = 60°C; melting point = 175°C.

Environmental pollution may be caused by waste polymers. To reduce such an impact and save oil resources, use of PLA and its modified derivatives may help, as it exhibits the following advantages: good compost, excellent performance, robust mechanical properties, and high transparency [3–5]. Its degradation products are often used in biomedical fields because they are nontoxic [6]. The carbon dioxide and water produced by the degradation can be returned to

nature [7, 8]; thus, the balance of carbon cycle on earth is maintained. The aforementioned descriptions render PLA to be one of the most useful biopolymers [9, 10].

PLA does possess good characteristics, but it has low heat resistance, inherent brittleness, slow crystallization rate, and poor dimensional stability. Hence, these disadvantages restrict its applications [11]. For this reason, PLA must be modified and properly toughened.

An efficient way of reinforcing the properties of PLA is to combine it with other polymers or additives through melt blending: polyester [12–16]; organic/inorganic fillers [17–19]; carbon nanotubes, nanosilica, montmorillonite, and graphene [20–24]. That would result in hybrid materials with better properties. Previous studies have reported the fabrication of several nanocomposites based on PLA.

Attapulgite (ATT) has good properties such as unique dispersion; excellent temperature resistance; great saline-alkali resistance; high adsorption and decoloration ability. It has certain plasticity and bond-

Table 1. Amounts of PLA and components of PLA/ATT blends

Sample	PLA, g	ATT, g
PLA	50.0	0.0
PLA ₉₅ ATT ₅	47.5	2.5
PLA ₉₀ ATT ₁₀	45.0	5.0
PLA ₈₅ ATT ₁₅	42.5	7.5
PLA ₈₀ ATT ₂₀	40.0	10.0

ing force, which make ATT widely used in all walks of life [25–29].

In recent years, incorporating ATT into composites has been examined. Yin et al. [30] prepared a novel ATT/biochar nanocomposite by simultaneous activation and carbonization processes. Zhang et al. [31] employed a straightforward method to synthesize nanocomposites of Cu/TiO₂/organo-ATT fiber. Then, they applied them to degrade acetone in the presence of air by subjecting it to ultraviolet light irradiation, a process also known as photocatalysis. Sun et al. [19] developed a composite adsorbent made from a porous ATT modified with chitosan. The response of such an adsorbent was really fast, and the composite itself was friendly to the environment and had demonstrated great utility in the field of potable water production. Gao et al. [32] polymerized ATT-modified 3-methacryloxypropyltrimethoxysilane with acrylic acid by the free radical approach and fabricated PLA/ATT nanocomposites. Liu et al. [33] was able to improve the elongation at the break of PLA/ATT nanocomposites by introducing 1–3% ATT to PLA, but the effect of increasing the amounts of ATT was to decrease the tensile strength. Ying et al. [34] demonstrated that ATT could strengthen PLA composites containing poly(butylene adipate-co-terephthalate) (PBAT). They indicated that 2.5 wt % ATT was uniformly dispersed in PBAT/PLA composites, which exhibited excellent tensile strength and toughness. However, there are very few studies on PLA matrices containing ATT. Also, high content of ATT must be explored.

This prompted us to determine the effect of adding varying amounts of ATT nanoparticles (5–20 wt %) to biodegradable PLA on the performance of the resultant nanocomposites. The effect was also evaluated on morphology, mechanical and thermal properties. PLA/ATT nanocomposites exhibited improved properties and performance.

EXPERIMENTAL

Materials

A 2002D grade of PLA, with a number weight molecular weight of 10⁴ g/mol, was used in this present study, and it was distributed by Nature works LLC (Minnesota, USA). PLA was synthesized by two-step processes. Firstly, the lactic acid was converted into cyclic dimer lactide, and then the ring opening polycondensation was carried out to form polylactic acid [35]. ATT, used as a reinforcing filler, came from Precision Chemical Co., Ltd, (Shanghai, China). It was the product of montmorillonite after alkali transformation, and its appearance and structure were fibrous. It had a large amount of SiO₂, MgO, Al₂O₃, other elements, and OH hydrophilic groups. Sodium hexametaphosphate (SHMP) ($M_n = 611.77$ g/mol) was purchased from HANAWA (Kazuno, Japan) and used to purify ATT.

Preparation of Purified Attapulgite

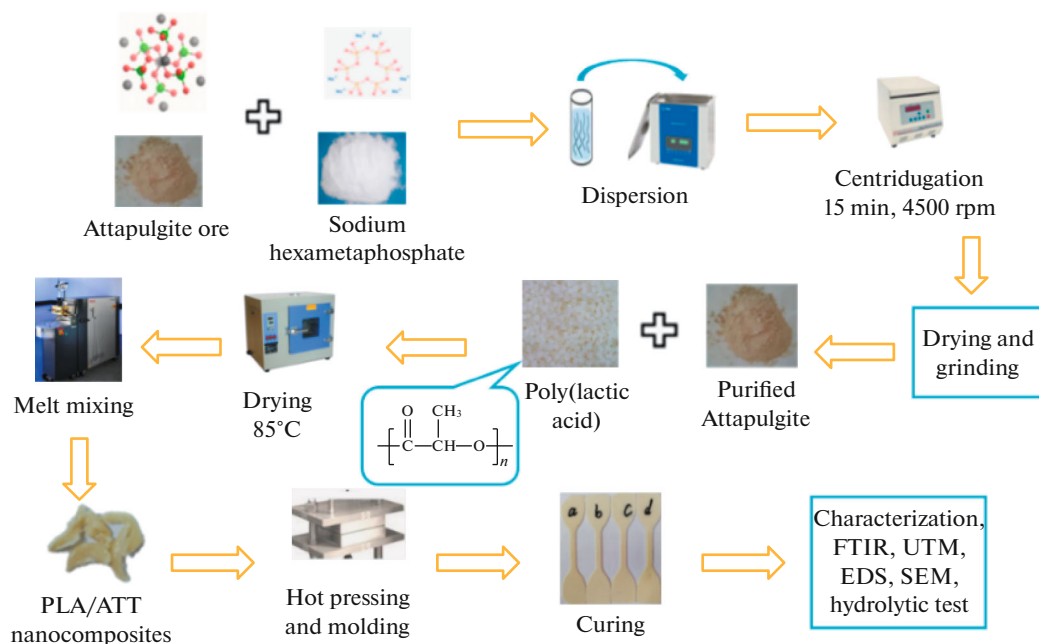
The first step was the dissolution of SHMP (0.6 g) in distilled water (400 mL). Then, ATT (20 g) was added to the aqueous SHMP solution and subsequently dispersed using ultrasonication for 10 h. Afterward, the solution was placed in a centrifuge machine. The centrifugation conditions were 15 min and 4500 rpm. Three layers appeared in the centrifuge tube. Water surged in the upper layer, while impurities settled in the lower layer, and the purified ATT stayed in the middle layer. The purified ATT was placed in an oven and dried at 80°C to form flakes that were later subjected to grinding.

Fabrication of PLA Nanocomposites Filled with ATT

First, it was necessary to dry both PLA and purified ATT for 8 h in a vacuum oven set at 85°C. Then, a method of melt compounding was employed to prepare nanocomposites of PLA filled with ATT whose concentration was varied: 0, 5, 10, 15, and 20 wt % (Table 1). For this melt compounding, a torque rheometer (PLE-331, BRABENDER) was operated at 120 rpm and 180°C for 5 min. Ultimately, the obtained nanocomposites of PLA containing ATT, as well as pure PLA, were formed into dumbbell shapes on a hot press. These samples in the form of dumbbells were used for tensile measurements. Scheme 1 diagrams the fabrication of PLA/ATT nanocomposites.

Characterization and Testing

The chemical structure of PLA/ATT nanocomposites was analyzed with a Fourier transform infrared spectrophotometer (Spectrum RXI FTIR, Perkin



Scheme 1.

Elmer, Massachusetts, USA), with the wave number ranging from 4000 to 500 cm^{-1} and scanning of 15 times.

Hot-pressed samples of pristine PLA and nanocomposites of PLA filled with varying amounts of ATT were measured for tensile strength and elongation at break by using a universal pull test machine (model ASTM D638, Shenzhen, China). Dumbbell sheets of different dimensions (length = 100 mm; width = 10 mm) were subjected to tensile tests. The sample preparation was based on the ASTM D638 Type IV standard. For each trial, at least five samples were measured to obtain representative average values of elongation at break and tensile strength.

Nanocomposites of PLA incorporated with ATT were examined for the elemental composition through energy dispersive spectroscopy (EDS, Bruker Instrument Co., Ltd, Karlsruhe, Germany).

To determine the thermogravimetric properties of nanocomposites of PLA into which ATT was added, thermogravimetric analysis (Pyris 1 TGA, Perkin Elmer, Massachusetts, USA) was conducted.

The cross-sectional images of PLA/ATT nanocomposites were captured using scanning electron microscopy (SEM, HITACHI, S-3400N, Tokyo, Japan). Prior to taking SEM images, the samples were initially coated a thin layer of gold.

Hydrolytic degradation measurements were carried out, where the medium used was distilled water, which was conditioned at the outset to have a pH equal to 7. Samples were weighed, then subjected to hydrolytic degradation by soaking them in distilled water. The

weight loss during the degradation process was monitored. The variation in residual weight fraction (Φ) as a function of the hydrolytic degradation time was then graphed. Herein, Φ was evaluated from the following equation [36]:

$$\Phi = W_0/W_t \times 100\%,$$

where W_0 represented the sample initial weight (g) (before the hydrolytic degradation) and W_t the residual weight (g) at a certain time (t) during the hydrolytic degradation. During the hydrolytic degradation process, the hydrolysis medium (distilled water) was unaffected, so it was possible to monitor the change in the nanocomposite concentration over the course of hydrolysis.

RESULTS AND DISCUSSION

Surface Chemical Structure

Figure 1 represents the FTIR spectral curves for PLA, ATT, and PLA/ATT nanocomposites. The PLA spectrum exhibited three absorption bands (1747, 2987, 3510 cm^{-1}), each of which described certain functional groups (motions of C=O bending, CH aliphatic stretching, OH stretching vibrations). The bending and asymmetric stretching vibrations of Si=O in ATT were identified at 987 and 1032 cm^{-1} absorption peaks, respectively [35]. Whereas, the absorption peak at 1444 cm^{-1} was attributed to the stretching vibrations of Mg=O groups in ATT.

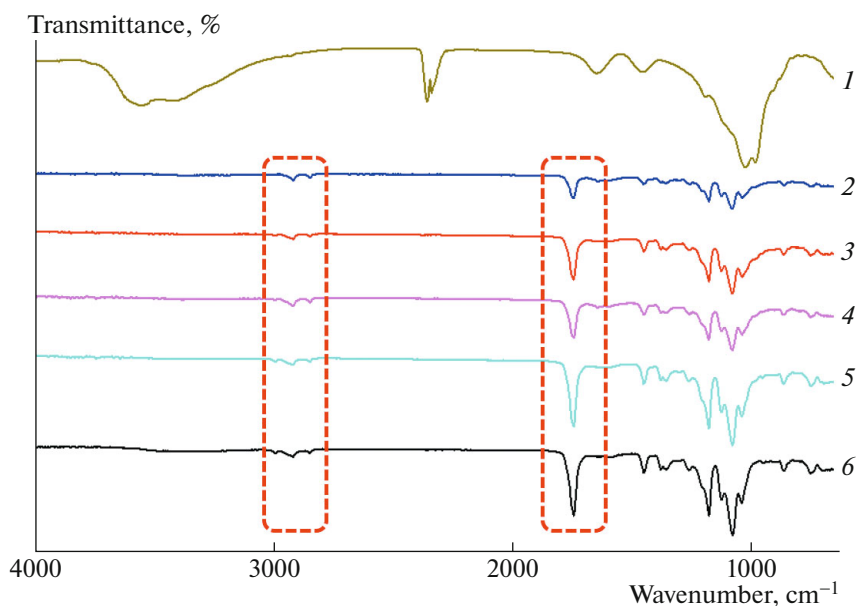


Fig. 1. FTIR spectra of (1) ATT, PLA/ATT nanocomposites: (2) PLA₈₀ATT₂₀, (3) PLA₈₅ATT₁₅, (4) PLA₉₀ATT₁₀, (5) PLA₉₅ATT₅, and (6) pristine PLA.

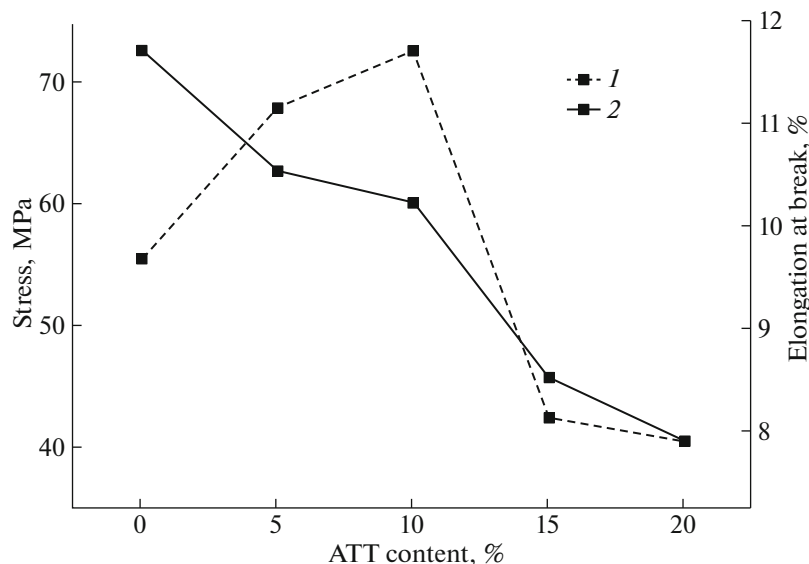


Fig. 2. (1) Stress and (2) elongation at break of PLA/ATT nanocomposites.

With increasing amounts of ATT, the peak (1747 cm^{-1}) originally shown in the FTIR spectrum of PLA, corresponding to the motion associated with the ester carbonyl (polyester C=O) stretching vibration, lessened in intensity. During the melt-blending of PLA/ATT nanocomposites, the carboxylic acid groups of PLA molecules reacted with the hydroxyl groups of ATT, the effect of which might be responsible for the decreased C=O bending absorption band (1747 cm^{-1}) [37].

Mechanical Properties

Figure 2 plots the stress and elongation at break of pristine PLA and PLA/ATT nanocomposites; Table 2 lists the data. The curve for tensile stress exhibited a maximum value at 10 wt% ATT. Beyond the optimum content, ATT started to agglomerate; thus, the nanocomposite strength began to decrease and eventually dipped sharply at much higher amounts of ATT, to the point that the nanocomposite had a lower strength than pristine PLA at 15 and 20 wt% ATT.

Table 2. Data on stress and elongation at break of pristine PLA and PLA/ATT nanocomposites

Sample	Stress, MPa	Elongation at break, %
PLA	54.5 ± 1.3	11.60
PLA ₉₅ ATT ₅	66.9 ± 1.9	10.43
PLA ₉₀ ATT ₁₀	71.6 ± 2.4	10.12
PLA ₈₅ ATT ₁₅	41.4 ± 4.8	8.41
PLA ₈₀ ATT ₂₀	39.5 ± 4.1	7.79

It can be observed from Fig. 2 that the tensile stress gradually increased to a maximum value when ATT was 10 wt %. Then, as the ATT content further increased, the tensile strength substantially decreased, because ATT would agglomerate and the strength of PLA changed. When the ATT content was 15 and 20 wt %, the nanocomposite was significantly lower in strength than pure PLA, which indicated that ATT may aggregate and lead to greater number of stress concentration points in the polymer matrix, ultimately resulting in undesirable mechanical properties [34, 38]. On the other hand, the elongation at break continually dropped with

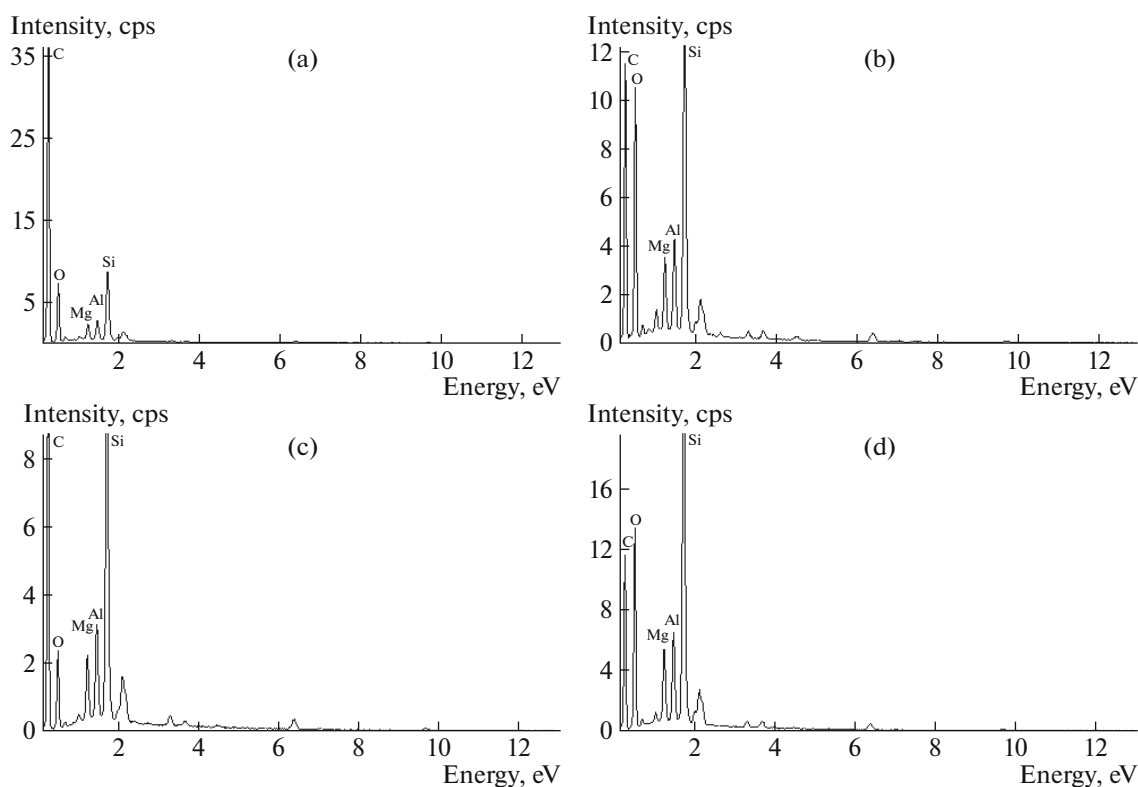
Table 3. Elemental composition of PLA/ATT nanocomposites

Sample	Si, wt %	Mg, wt %	Al, wt %
PLA ₉₅ ATT ₅	5.48	1.21	1.45
PLA ₉₀ ATT ₁₀	12.93	2.60	3.31
PLA ₈₅ ATT ₁₅	14.11	2.57	3.69
PLA ₈₀ ATT ₂₀	17.09	3.18	3.89

increasing amounts of ATT, until the value was even lower than that of pure PLA.

Elemental Content

Table 3 summarizes the elemental composition of PLA/ATT nanocomposites. Figure 3 presents the energy dispersive spectra of different nanocomposites, depending on the content of ATT in PLA. The content of the three elements (Si, Mg, Al) in the case of ATT₅PLA₉₅ was relatively low (Fig. 3a); whereas, the content was higher for ATT₁₀PLA₉₀ (Fig. 3b), ATT₁₅PLA₈₅ (Fig. 3c), and ATT₂₀PLA₈₀ (Fig. 3d).

**Fig. 3.** Analysis of energy dispersive spectroscopy for PLA/ATT nanocomposites: (a) PLA₉₅ATT₅, (b) PLA₉₀ATT₁₀, (c) PLA₈₅ATT₁₅, (d) PLA₈₀ATT₂₀.

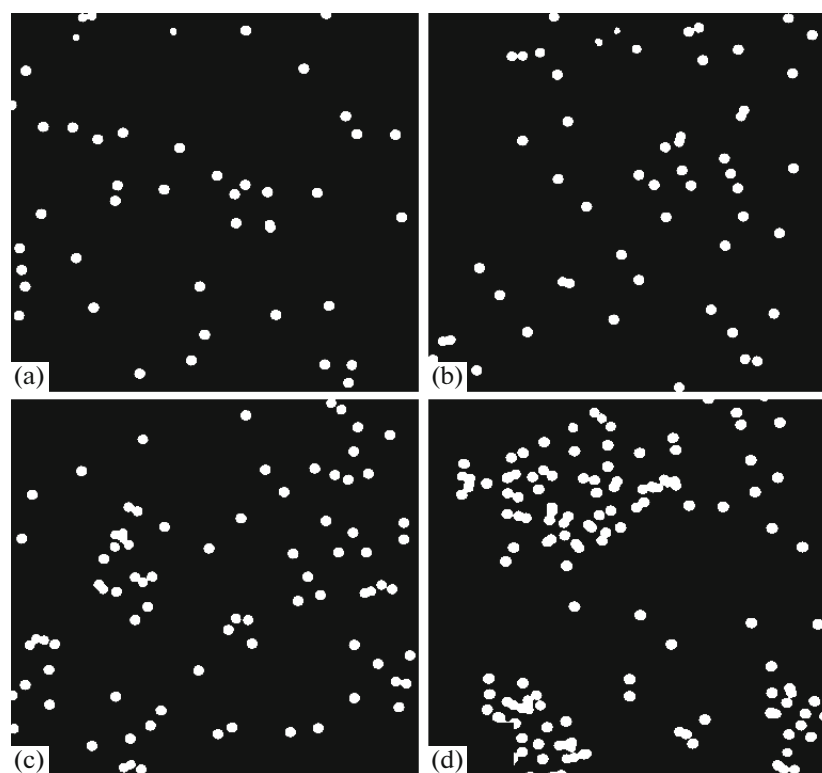


Fig. 4. Distribution of silicon in PLA/ATT nanocomposites: (a) PLA₉₅ATT₅, (b) PLA₉₀ATT₁₀, (c) PLA₈₅ATT₁₅, (d) PLA₈₀ATT₂₀. Si-K.

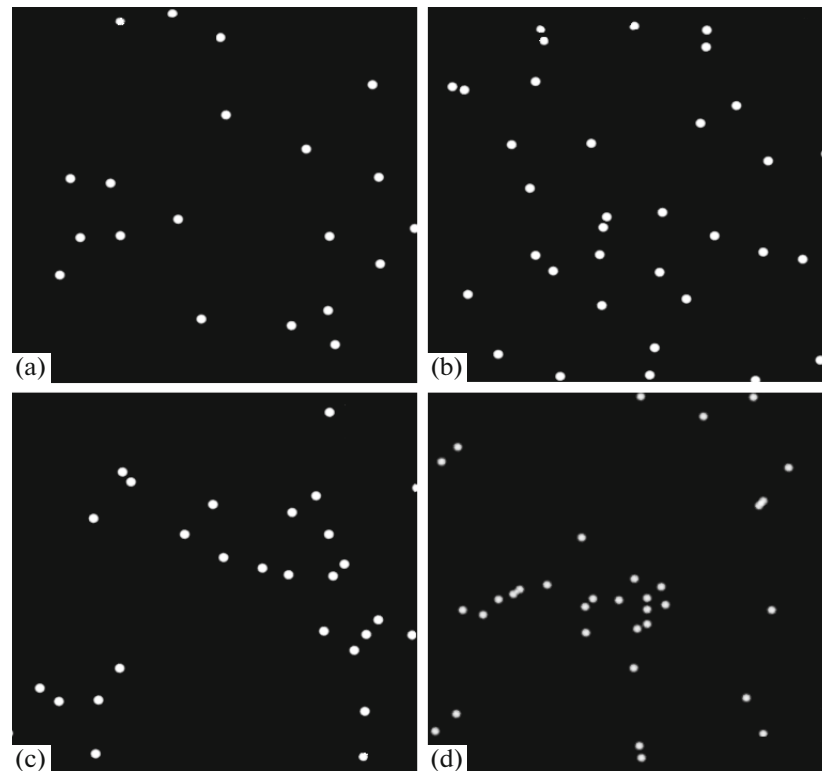


Fig. 5. Distribution of magnesium in PLA/ATT nanocomposites: (a) PLA₉₅ATT₅, (b) PLA₉₀ATT₁₀, (c) PLA₈₅ATT₁₅, (d) PLA₈₀ATT₂₀. Mg-K.

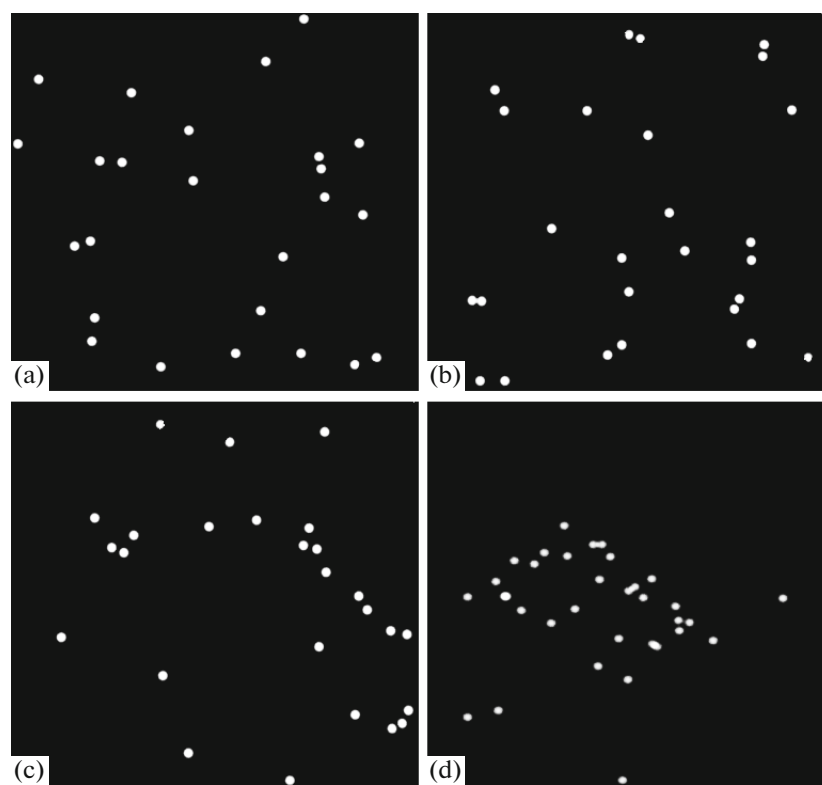


Fig. 6. Distribution of aluminum in PLA/ATT nanocomposites: (a) PLA₉₅ATT₅, (b) PLA₉₀ATT₁₀, (c) PLA₈₅ATT₁₅, (d) PLA₈₀ATT₂₀. Al-K.

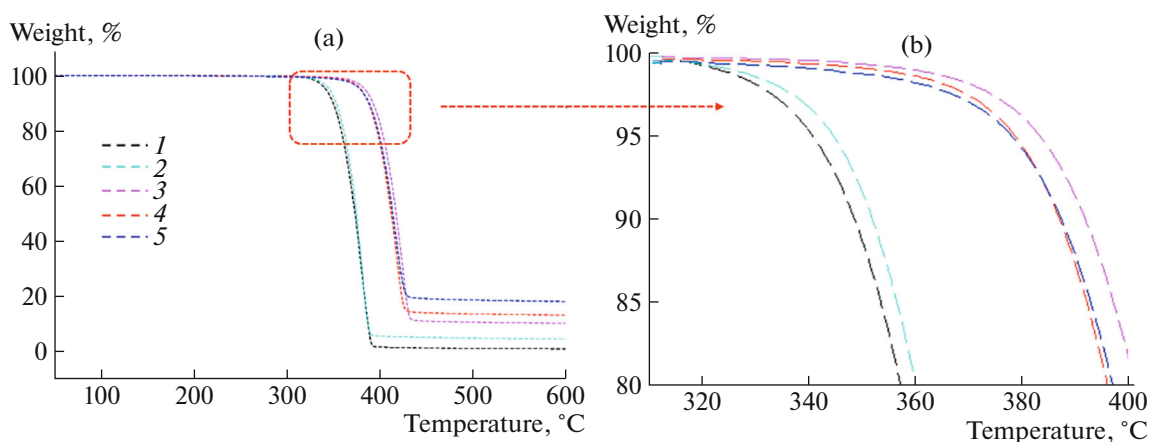


Fig. 7. Thermogravimetric analysis for PLA/ATT nanocomposites with different ATT content: (1) PLA, (2) PLA₉₅ATT₅, (3) PLA₉₀ATT₁₀, (4) PLA₈₅ATT₁₅, (5) PLA₈₀ATT₂₀.

Figures 4–6 illustrate the distribution of the three elements in the different nanocomposites. The distribution was uniform when the content of ATT was 5–10 wt % (Figs. 4a, 4b, 5a, 5b, 6a, 6b). However, aggregation of ATT occurred when the content was

15–20 wt % (Figs. 4c, 4d, 5c, 5d, 6c, 6d). These EDS data provide explanations to the tensile properties discussed in Section “Mechanical properties”. In EDS analysis, the total content of ATT element is slightly higher than the actual value, because the sen-

Table 4. Thermogravimetric data for pure PLA and its nanocomposites with different amounts of ATT

Sample	Initial decomposition temperature, °C	Residual amount, % (600°C)
PLA	350.3	0.9
PLA ₉₅ ATT ₅	364.5	4.8
PLA ₉₀ ATT ₁₀	400.7	10.5
PLA ₈₅ ATT ₁₅	395.8	13.4
PLA ₈₀ ATT ₂₀	394.5	18.3

sitivity of EDS equipment to the elements of polymer substrate itself is lower. The results show that the content of ATT increases with the increase of nano fillers.

Thermogravimetric Properties

Figure 7a shows the thermal decomposition of PLA/ATT nanocomposites, whereas Fig. 7b indicates the thermal stability. The TGA results demonstrated that the incorporation of an optimal amount of ATT could considerably improve the thermal stability of the PLA/ATT nanocomposites [39, 40]. Table 4 summarizes the data on the initial decomposition temperature and thermal weight loss of PLA/ATT nanocom-

posites. The residual yield of the nanocomposites increased with the ATT content, indicating that the thermal decomposition of the polymer matrix was impeded.

Morphology

Fillers when dispersed in a polymer matrix affect the mechanical properties of nanocomposites in a considerable way [41, 42]. If ATT is dispersed well in a polymer matrix, and the ensuing interfacial adhesion between them is strong, then the resultant nanocomposite would have satisfactory mechanical properties [43, 44]. Scanning electron microscopy (SEM) was considered to provide an analysis of the surface morphology of fractured PLA/ATT nanocomposites with different amounts of ATT. Figure 8 shows the SEM microphotographs. In Fig. 8a, the surface of pure PLA was smooth [45–47]. In the presence of ATT, however, the nanocomposite surface became completely different from that of pure PLA; the surface roughness increased with the content of ATT (Figs. 8b–8e). ATT was dispersed well in the polymer matrix when the ATT concentration was as high as 10 wt %, but agglomerates formed at higher concentrations of 15–20 wt % ATT [48]. ATT was dispersed well in ATT₁₀PLA₉₀, suggesting that a strong interfacial interaction existed between ATT and PLA. When PLA was filled with 15–20 wt % ATT, agglomeration of fillers

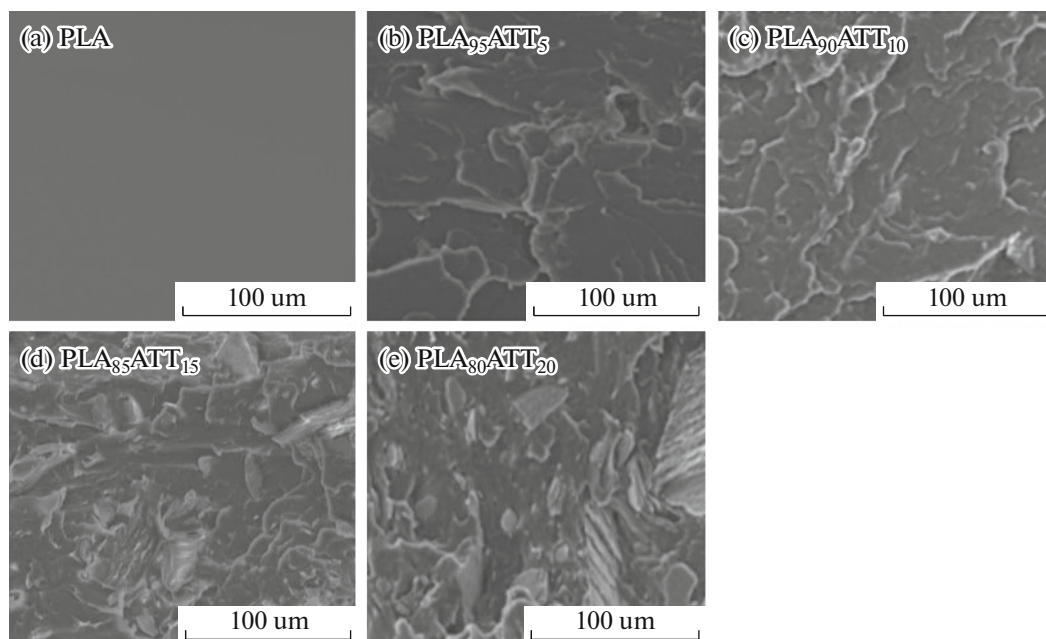


Fig. 8. Surface SEM micrographs of fractured PLA/ATT nanocomposites with various amounts of ATT: (a) PLA, (b) PLA₉₅ATT₅, (c) PLA₉₀ATT₁₀, (d) PLA₈₅ATT₁₅, (e) PLA₈₀ATT₂₀.

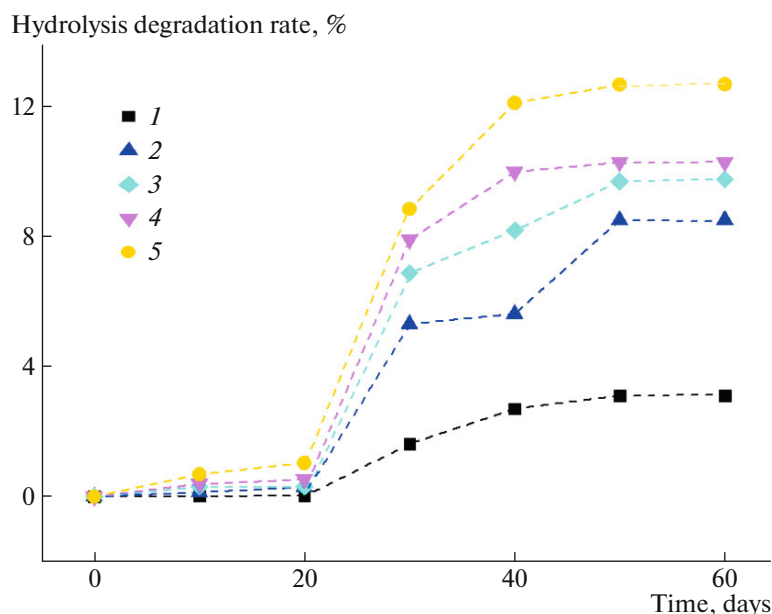


Fig. 9. Hydrolysis degradation rate of samples as function of hydrolysis degradation time: (1) PLA, (2) PLA₉₅ATT₅, (3) PLA₉₀ATT₁₀, (4) PLA₈₅ATT₁₅, (5) PLA₈₀ATT₂₀.

persisted, and that condition decreased the interfacial adhesion between ATT and PLA. Again, the results pertaining to aggregation described in tensile strength, EDS, and TGA were verified.

Hydrolytic Degradation

Figure 9 illustrates how the hydrolysis degradation rates varied with different periods of hydrolysis degradation time for pristine PLA and various PLA/ATT nanocomposites. The process of degradation can be categorized into two stages: initial stage (Stage I) for a period <30 days, and final stage (Stage II) for >30 days. Hydrolysis degradation rates did not change much in Stage I. In Stage II, however, changes were

apparent, signifying greatly increased degradation rates (i.e., all samples displayed ‘self-accelerating effect’ over the course of the hydrolysis degradation process [49]).

The images in Figs. 10a–10e illustrate the increasingly apparent degree of hydrolysis in the samples of varying content of ATT at the same degradation time. The degradation rate was considerably faster with the nanocomposite with higher concentrations of ATT. Because water infiltrated into the polymer matrix, the polymer molecular chains relaxed, ester bond underwent hydrolysis, molecular weight was reduced, and a gradual degradation occurred to produce an oligomer. With the degradation of samples in Stage II, increasingly more carboxyl groups would speed up the inter-

Table 5. Hydrolysis rate of PLA and PLA/ATT nanocomposites at 37°C

Day	PLA	PLA ₉₅ ATT ₅	PLA ₉₀ ATT ₁₀	PLA ₈₅ ATT ₁₅	PLA ₈₀ ATT ₂₀
0	0	0	0	0	0
10	0.0287 ± 0.0002	0.1392 ± 0.0001	0.2964 ± 0.007	0.3935 ± 0.004	0.6890 ± 0.0015
20	0.0367 ± 0.0009	0.2915 ± 0.0014	0.3030 ± 0.0026	0.5304 ± 0.0012	1.0340 ± 0.0048
30	1.6252 ± 0.0063	5.3107 ± 0.0771	6.8752 ± 0.0542	7.8935 ± 0.0482	8.8358 ± 0.0631
40	2.7037 ± 0.0137	5.6122 ± 0.0572	8.1868 ± 0.0352	9.9842 ± 0.0835	12.0952 ± 0.0259
50	3.1069 ± 0.0247	8.5012 ± 0.0247	9.6843 ± 0.0594	10.2769 ± 0.0958	12.6624 ± 0.1571
60	3.1168 ± 0.0925	8.5122 ± 0.0759	9.7422 ± 0.1353	10.2811 ± 0.0752	12.6724 ± 0.1235

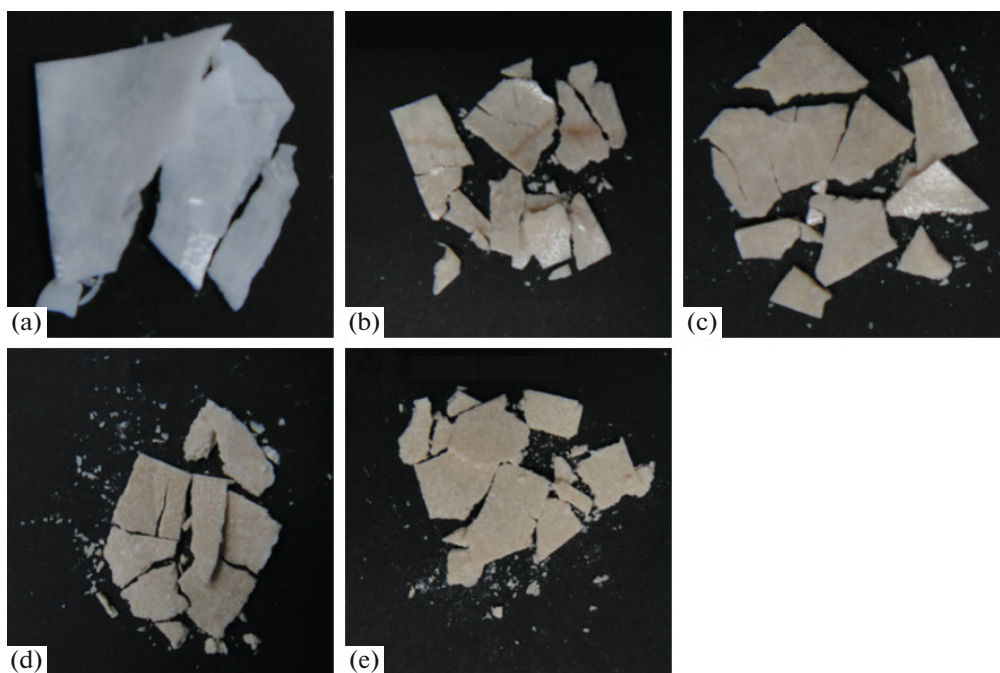


Fig. 10. Digital images of (a) PLA and PLA/ATT: (b) PLA₉₅ATT₅, (c) PLA₉₀ATT₁₀, (d) PLA₈₅ATT₁₅, (e) PLA₈₀ATT₂₀ after 50 days of hydrolysis.

nal degradation, leading to increased degradation of oligomer that hydrolyzed to small molecules, which ultimately dissolved in water (employed as medium). The hydrolytic degradation of PLA-based composites could proceed by two different mechanisms: (1) surface or heterogeneous reactions and (2) bulk or homogeneous erosion [50, 51]. Some researchers also indicated that hydrolytic degradation must reduce molecular weight of PLA to $(1.5-4.0) \times 10^4$ before biodegradation could take over [52]. Li et al. indicated that the change in the molar mass distribution and surface morphology of the blend composites after hydrolysis demonstrated that the hydrolytic degradation proceeds homogeneously via bulk erosion mechanism [53]. As a result, cracks in the sample were observed macroscopically at day 50, and the cracks increased with the concentration of ATT in the sample. Figure 9 shows that after more than 50 days of degradation time, the nanocomposite almost no longer degraded. It might be due to ATT is alkaline and neutralizes the acidity of PLA degradation products, the autocatalytic effect is eliminated to a certain extent in the degradation process of PLA/ATT nanocomposite. Therefore, the degradation rate of PLA/ATT composite slows down with the increase of degradation time [54].

CONCLUSIONS

PLA/ATT nanocomposites were fabricated through a simple method of melt blending. ATT

reinforced the PLA polymer matrix. However, excessive ATT reduced the mechanical properties and thermal stability, because ATT aggregation was inevitable. PLA/ATT nanocomposites demonstrated enhanced hydrolysis degradation ability. The rate of hydrolysis degradation was affected by varying amounts of ATT and different periods of hydrolysis degradation time.

FUNDING

The authors would like to acknowledge the financial support from the following organizations: Wuliangye Group Co. Ltd. (CXY2019ZR001); Sichuan Province Science and Technology Support Program (2019JDRC0029); Zigong City Science and Technology (2017XC16; 2019CXRC01; 2022); Opening Project of Material Corrosion and Protection Key Laboratory of Sichuan Province (2019CL05; 2018CL08; 2020CL19; 2020CL21; 2020CL03); Opening Project of Sichuan Province, the Foundation of Introduced Talent of Sichuan University of Science and Engineering (2017RCL31; 2017RCL36; 2017RCL16; 2019RC05; 2019RC07). Appreciation is also extended to the National Natural Science Foundation of China; Apex Nanotek Co. Ltd.; Ratchadapisek Sompote Fund for Postdoctoral Fellowship (Chulalongkon University).

CONFLICT OF INTEREST

The authors declare that they have no conflict of interest.

REFERENCES

- C.-H. Tsou, W.-H. Yao, W.-S. Hung, M.-C. Suen, M. De Guzman, J. Chen, C.-Y. Tsou, R. Y. Wang, J.-C. Chen and C.-S. Wu, *Ind. Eng. Chem. Res.* **57**, 2537 (2018).
- V. Jašo, G. Glenn, A. Klameczynski, and Z. S. Petrović, *Polym. Test.* **47**, 1 (2015).
- S. M. Davachi, B. S. Heidari, I. Hejazi, J. Seyfi, E. Oli-aei, A. Farzaneh, and H. Rashedi, *Carbohydr. Polym.* **155**, 336 (2017).
- A. R. Kakroodi, Y. Kazemi, M. Nofar, and C. B. Park, *Chem. Eng. J.* **308**, 772 (2017).
- Y. N. Wang, Y. X. Weng, and L. Wang, *Polym. Test.* **36**, 119 (2014).
- K. A. Athanasiou, G. G. Niederauer, and C. M. Agrawal, *Biomaterials* **17**, 93 (1996).
- I. Armentano, N. Bitinis, E. Fortunati, S. Mattioli, N. Rescignano, R. Verdejo, and J. M. Kenny, *Prog. Polym. Sci.* **38**, 1720 (2013).
- F. L. Jin, R. R. Hu, and S. J. Park, *Composites, Part B* **25**, 1097 (2018).
- L. A. Granda, F. X. Espinach, Q. Tarrés, J. A. Méndez, M. Delgado-Aguilar, and P. Mutjé, *Composites, Part B* **99**, 514 (2016).
- R. Scaffaro, F. Lopresti, and L. Botta, *Composites, Part B* **139**, 1 (2018).
- R. M. Rasal, A. V. Janorkar, and D. E. Hirt, *Prog. Polym. Sci.* **35**, 338 (2010).
- J. G. Ausejo, J. Rydz, M. Musioł, W. Sikorska, M. Sobota, J. Włodarczyk, and B. Johnston, *Polym. Degrad. Stab.* **152**, 191 (2018).
- C. H. Tsou, B. J. Kao, M. C. Suen, M. C. Yang, T. Y. Wu, C. Y. Tsou, J.-C. Chen, W.-H. Yao, C.-K. Chu, X.-M. Tuan, J.-Z. Hwang, W.-S. Hung, K.-R. Lee, and J. Y. Lai, *Mater. Res. Innovations* **18**, S2372 (2014).
- C. H. Tsou, W. S. Hung, C. S. Wu, J. C. Chen, C. Y. Huang, S. H. Chiu, C. Y. Tsou, W. H. Yao, S. M. Lin, C. K. Chu, C. C. Hu, K. R. Lee, and M. C. Suen, *Mater. Sci.* **20**, 446 (2014).
- Y. Ding, W. Feng, B. Lu, P. Wang, G. Wang, and J. Ji, *Polymer* **146**, 179 (2018).
- C. Y. Tsou, C. L. Wu, C. H. Tsou, S. H. Chiu, M. C. Suen, and W. S. Hung, *Polym. Sci., Ser. B* **57**, 473 (2015).
- P. Chen, X. Liang, Y. Xu, Y. Zhou, and W. Nie, *Appl. Surf. Sci.* **440**, 1143 (2018).
- Y. Wen, C. H. Tsou, C. Gao, J. C. Chen, Z. Tang, and Z. Chen, *J. Polym. Res.* **27**, article no. 167 (2020). <https://doi.org/10.1007/s10965-020-02148-8>
- N. Sun, Y. Zhang, L. Ma, S. Yu, and J. Li, *J. Taiwan Inst. Chem. Eng.* **78**, 96 (2017).
- C. Kaynak and B. Sari, *Appl. Clay Sci.* **121**, 86 (2016).
- M. Nerantzaki, L. Prokopiou, D. N. Bikiaris, D. Patsiaoura, K. Chrissafis, P. Klonos, and P. Pissis, *Thermochim. Acta* **669**, 16 (2018).
- Y.-L. Yao, M. R. De Guzman, H. Duan, C. Gao, X. Lin, Y.-H. Wen, and C.-H. Tsou, *Chin. J. Polym. Sci.* **38**, 898 (2020). <https://doi.org/10.1007/s10118-020-2392-z>
- E. Picard, E. Espuche, and R. Fulchiron, *Appl. Clay Sci.* **53**, 58 (2011).
- C. H. Tsou, W. H. Yao, Y. C. Lu, C. Y. Tsou, C. S. Wu, J. Chen, R. Y. Wang, C. Su, W. S. Hung, M. De Guzman, and M. C. Suen, *Polymers* **9**, 100 (2017).
- J. M. Busnel, B. Schoenmaker, R. Ramautar, A. Carrasco-Pancorbo, C. Ratnayake, J. S. Feitelson, and O. A. Mayboroda, *Anal. Chem.* **82**, 9476 (2010).
- G. Zhu, L. Sun, and N. J. Dovichi, *Talanta* **146**, 839 (2016).
- R. A. Lubeckyj, E. N. McCool, X. Shen, Q. Kou, X. Liu, and L. Sun, *Anal. Chem.* **89**, 12059 (2017).
- J. Jiménez, M. E. Cisneros-Ortiz, Y. Guardia-Puebla, J. M. Morgan-Sagastume, and A. Noyola, *Water Sci. Technol.* **69**, 2381 (2014).
- H. Shi, M. Sun, Y. Yu, M. Shi, F. N. Shi, F. Liu, and E. H. Han, *Prog. Org. Coat.* **137**, 105347 (2019).
- Z. Yin, Y. Liu, X. Tan, L. Jiang, G. Zeng, S. Liu, and M. Li, *Process Saf. Environ. Prot.* **121**, 155 (2019).
- G. Zhang, H. Wang, S. Guo, J. Wang, and J. Liu, *Appl. Surf. Sci.* **362**, 257 (2016).
- D. Gao, Y. L. Zhang, B. Yu, P. Wang, and J. Ma, *Carbohydr. Polym.* **206**, 245 (2019).
- L. Liu, Y. Wang, Y. Zuo, Y. Jiang, and S. Han, *J. Chin. Ceram. Soc.* **40**, 1760 (2012).
- Z. Ying, L. Lei, B. Yang, J. Li, and J. Ren, *Polym. Test.* **60**, 78 (2017).
- M. M. Hassan, "Textile: Fibre-Forming Polymers," in *Encyclopedia of Polymer Applications*, Ed. by M. Mishra (CRC Press, Boca Raton, 2018), pp. 2490–2506. <https://doi.org/10.1201/9781351019422-140000360>
- N. Zhang, X. Yu, J. Duan, J. H. Yang, T. Huang, X. D. Qi, and Y. Wang, *Polym. Degrad. Stab.* **148**, 1 (2018).
- J. Xu, J. Zhang, W. Gao, H. Liang, H. Wang, and J. Li, *Mater. Lett.* **63**, 658 (2009).
- A. Kumar and V. R. Tumu, *Composites, Part B* **175**, 1095 (2019).
- C. H. Tsou, C. S. Wu, W. S. Hung, M. R. De Guzman, C. Gao, R. Y. Wang, and M. C. Suen, *Polymer* **160**, 265 (2019).
- C. H. Tsou, W. H. Yao, Y. C. Lu, C. Y. Tsou, C. S. Wu, J. Chen, M. C. Suen, *Polymer* **9**, 100 (2017).
- Z. Qi, H. Ye, J. Xu, J. Peng, J. Chen, and B. Guo, *Colloids Surf., A* **436**, 26 (2013).
- P. Dittanet and R. A. Pearson, *Polymer* **53**, 1890 (2012).
- P. Carballeira and F. Hauptert, *Polym. Compos.* **31**, 1241 (2010).
- H. Liu, W. Song, F. Chen, L. Guo, and J. Zhang, *Macromolecules* **44**, 1513 (2011).
- C. H. Tsou, W. H. Yao, C. S. Wu, C. Y. Tsou, W. S. Hung, J. C. Chen, J. Guo, S. Yuan, E. Wen, R. Y. Wang, M. C. Suen, S. C. Liu, and M. R. De Guzman, *J. Polym. Res.* **26**, article no. 227 (2019). <https://doi.org/10.1007/s10965-019-1882-6>

46. C. S. Wu and C. H. Tsou, *J. Polym. Res.* **26**, 44 (2019).
47. C. H. Tsou, M. C. Suen, W. H. Yao, J. T. Yeh, C. S. Wu, C. Y. Tsou, S. H. Chiu, J. C. Chen, R. Y. Wang, S. M. Lin, M. S. Hung, M. De Guzman, and K. R. Lee, *Materials* **7**, 5617 (2014).
48. C. H. Tsou, C. S. Wu, W. S. Hung, M. R. De Guzman, C. Gao, R. Y. Wang, J. Chen, N. Wan, Y. J. Peng, and M. C. Suen, *Polymer* **160**, 265 (2019).
49. X. Wang, J. Li, and L. Zhang, *Chin. J. Chem. Eng.* **27**, 759 (2019).
50. M. A. Elsayy, K.-H. Kim, J.-W. Park, and A. Deep, *Renewable Sustainable Energy Rev.* **79**, 1346 (2017).
51. J. Siepmann, *Adv. Drug Delivery Rev.* **48**, 229 (2001).
52. R. A. Cairncross, J. G. Becker, S. Ramaswamy, and R. O'connor, *Appl. Biochem. Biotechnol.* **131**, 774 (2006).
53. S. Li and Y. Hu, "Chapter 2: Polylactid Stereo-complex: From Principles to Applications," in *Poly(lactic acid) Science and Technology. Processing, Properties, Additives and Applications*, Ed. by A. Jiménez, M. Peltzer, and R. Ruseckaite (Royal Society of Chemistry, London, 2014), pp. 45–59.
54. T. Bansagi, and A. F. Taylor, *Tetrahedron* **73**, 5018 (2017).